

High-Power Hydro-Actuators Fabricated from Biomimetic Carbon Nanotube Coiled Yarns with Fast Electrothermal Recovery

Wonkyeong Son,[△] Jae Myeong Lee,[△] Shi Hyeong Kim, Hyeon Woo Kim, Sung Beom Cho, Dongseok Suh, Sungwoo Chun,* and Changsoon Choi*



Cite This: *Nano Lett.* 2022, 22, 2470–2478



Read Online

ACCESS |

Metrics & More

Article Recommendations

Supporting Information

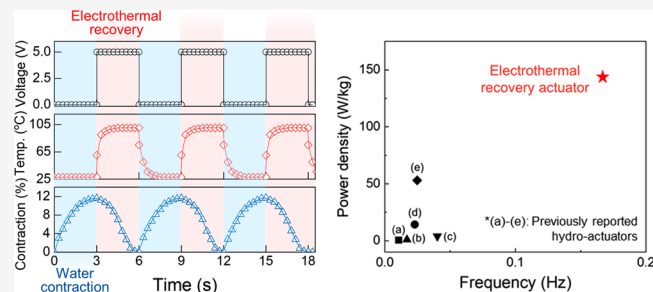
ABSTRACT: Bioinspired yarn/fiber structured hydro-actuators have recently attracted significant attention. However, most water-driven mechanical actuators are unsatisfactory because of the slow recovery process and low full-time power density. A rapidly recoverable high-power hydro-actuator is reported by designing biomimetic carbon nanotube (CNT) yarns. The hydrophilic CNT (HCNT) coiled yarn was prepared by storing pre-twist into CNT sheets and subsequent electrochemical oxidation (ECO) treatment. The resulting yarn demonstrated structural stability even when one end was cut off without the possible loss of pre-stored twists. The HCNT coiled yarn actuators provided maximal contractile work of 863 J/kg at 11.8 MPa stress when driven by water. Moreover, the recovery time of electrically heated yarns at a direct current voltage of 5 V was 95% shorter than that of neat yarns without electric heating. Finally, the electrothermally recoverable hydro-actuators showed a high actuation frequency (0.17 Hz) and full-time power density (143.8 W/kg).

KEYWORDS: power density, hydro-actuator, biomimetics, carbon nanotube yarn, electrothermal recovery

INTRODUCTION

Motility is an intrinsic feature of living things in nature. The motions of a plant, which differ from those of an animal, have evolved to diverse types such as bending, twisting, and contracting based on the internal helical structure.^{1,2} These motions rely on the swelling and shrinking of plant cells in response to ambient humidity^{2–5} and play essential roles in their survival.⁶ Recently, plant-inspired, water-responsive yarn/fiber-based actuators have been an active research field because of the outstanding actuation stroke and work capacity; in addition, they do not require an external energy system.⁷ Some pioneering researchers have employed natural fibers such as silk, wool, and cotton^{8–11} since they consist of amino acids or cellulose with hydrophilic functional groups.¹² Carbon nanomaterials (e.g., graphene, carbon nanotubes (CNTs)), which have widely been used for yarn/fiber-based actuators,^{13–20} are promising candidates because of their excellent mechanical and electrical properties. The key mechanism of hydro-actuators is water absorption-induced yarn volume expansion. Thus, one has obtained water-responsive carbon-based actuators by introducing amphiphilic substances or modifying their surfaces with oxygen plasma or acid treatments.^{21–24}

Unfortunately, existing hydro-actuators share a critical issue of long recovery time. Previously reported hydro-actuators provided fast contraction time (the time required to reach stable contraction state); however, the recovery time (the time required to return to the original state) was up to 50 times the



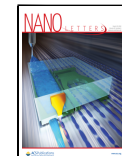
contraction time.^{25–28} Ironically, a hydrogen bond with water, provided by the hydrophilicity of actuators, is the main factor that hinders the effective evaporation of trapped water²¹ and significantly extends the recovery time for actuator relaxation. Because of this largely extended recovery time, both the actuation frequency (the reciprocal of the total cycle time for actuator contraction and relaxation, which also means the number of actuation cycles per unit time) and full-time power density (the ratio of the contraction work capacity to the total cycle time¹⁹) of the hydro-actuators are much lower (<0.05 Hz and <50 W/kg, respectively) than those of actuators powered by electrochemical, thermal, and photonic stimuli.^{13,14,18} Thus, the limitation of the long recovery time issue of the hydro-actuators needs to be solved for practical applications in which fast repeated actuation and a high output power are required.

Electric heating method (a process in which the electric energy applied to a conductor is converted into thermal energy) can be a promising solution to shorten the recovery time of the hydro-actuators because water evaporation can be dramatically accelerated by generated heat, irrespective of the

Received: January 20, 2022

Revised: March 1, 2022

Published: March 7, 2022



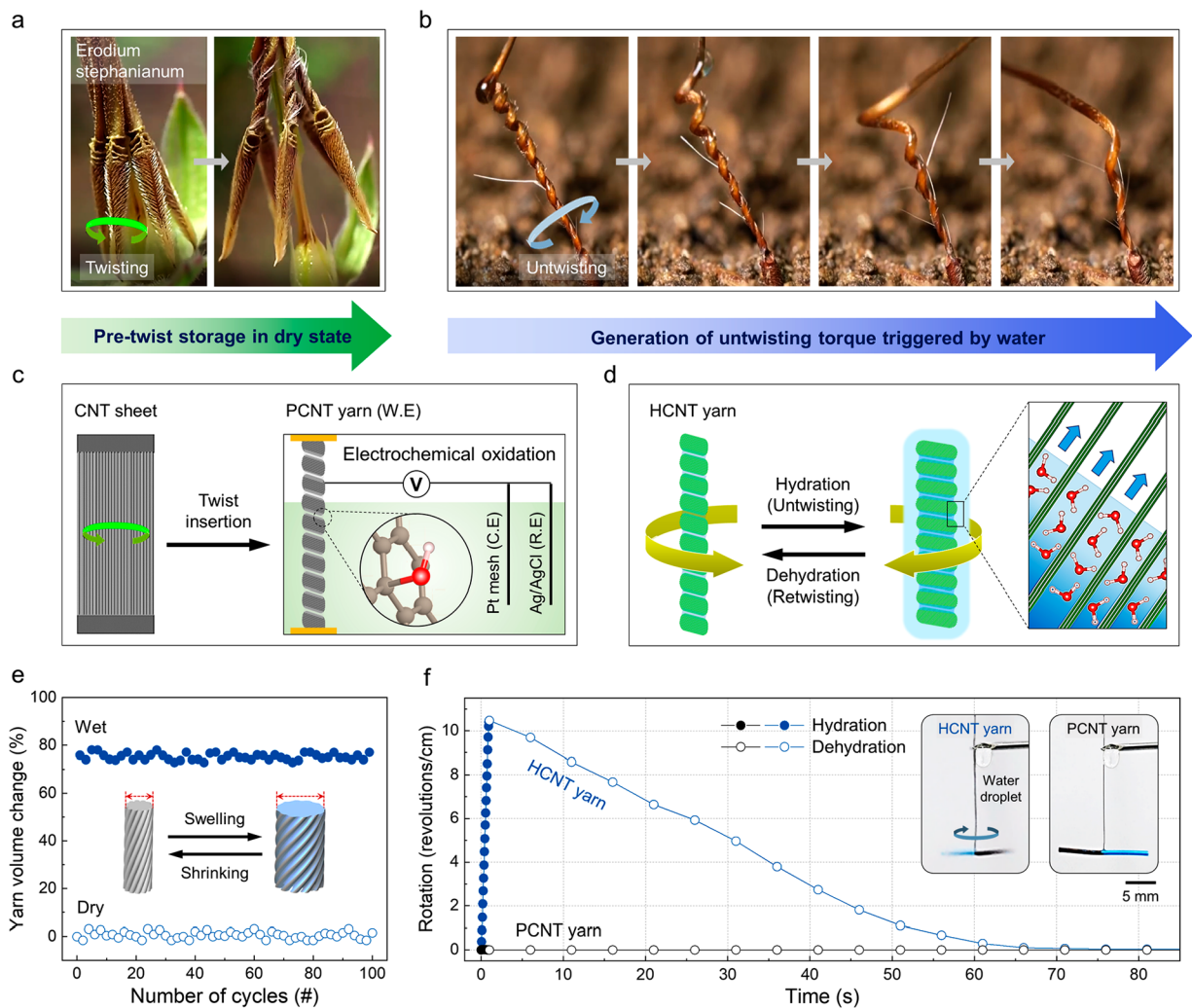


Figure 1. Concept and strategy to fabricate biomimetic carbon nanotube (CNT) yarn-based hydro-actuators. (a) Photographs show self-twisting motion of an awn of *Erodium stephanianum* in the dry state.⁴⁴ (b) Untwisting movement of the seed awn triggered by raindrops from a initially dry, twisted configuration.⁴⁴ (c) Schematics show the pre-twisting process from an aligned CNT sheet to a pristine CNT (PCNT) coiled yarn and the configuration for electrochemical oxidation (ECO) treatment setup consisting of a CNT yarn working electrode and counter (Pt mesh) and reference (Ag/AgCl) electrodes in an aqueous electrolyte (0.1 M Na₂SO₄). Inset shows the molecular structure of the CNT yarn surface functionalized with hydroxyl groups by ECO treatment. (d) Schematics show untwisting and retwisting actuation of a hydrophilic CNT (HCNT) coiled yarn when driven by absorption (hydration) and desorption (dehydration) of water, respectively. Inset shows the enlarged view of the water infiltration through the nanochannels (arrows) of the aligned CNTs. (e) Volume changes (%) of HCNT yarns during 100 repeated water absorption and desorption cycles. Insets show swelling and shrinking HCNT yarns during water absorption and desorption, respectively. (f) Time dependence of torsional stroke of PCNT and HCNT yarns upon the alternation of hydration and dehydration. Insets show PCNT and HCNT yarns with a heavy paddle when in contact with a water droplet. Left inset image: hanging paddle was stationary. Right inset image: torsional actuation generated during water diffusion along the yarn. The paddle weight was 10 mg.

external environmental conditions such as the atmospheric temperature and relative humidity. According to Joule's first law ($P = VI = V^2/R$), electric heating with a direct current (DC) voltage needs target materials with high electrical conductivity for high electricity to heat efficiency. Unfortunately, the heavily hydrophilized carbon nanomaterials of previous hydro-actuators have poor electrical conductivity due to severely damaged sp² carbon networks; electric heating approach has been barely applicable for them. Therefore, hydrophilized carbon nanomaterials with high electrical conductivity will be promising material candidates to obtain high-power hydro-actuators for practical applications.

This research presents electrothermally recoverable hydro-actuators with high actuation frequencies and high power densities due to electrochemically oxidized CNT coiled yarns.

The contents of functional groups in the hydrophilic CNTs (HCNTs) were adjusted via a facile electrochemical oxidation (ECO) treatment;^{29,30} the conductivity of HCNTs improves the dehydration rate in electric heating. After 12% water-driven contraction at 11.8 MPa stress, the HCNT coiled yarn hydro-actuator was heated to 105 °C with a 5 V voltage; this step reduced the full cycle time by 95% (6 s) compared to that of naturally recovered yarn (120 s). This resulted in a high actuation frequency (0.17 Hz) and high full-time power density (143.8 W/kg), which are the highest reported values for hydro-actuators so far. High-power hydro-actuators with fast electrothermal recovery are expected to be used in diverse applications, including exoskeletons, robot arms, and smart wearable devices in the future.

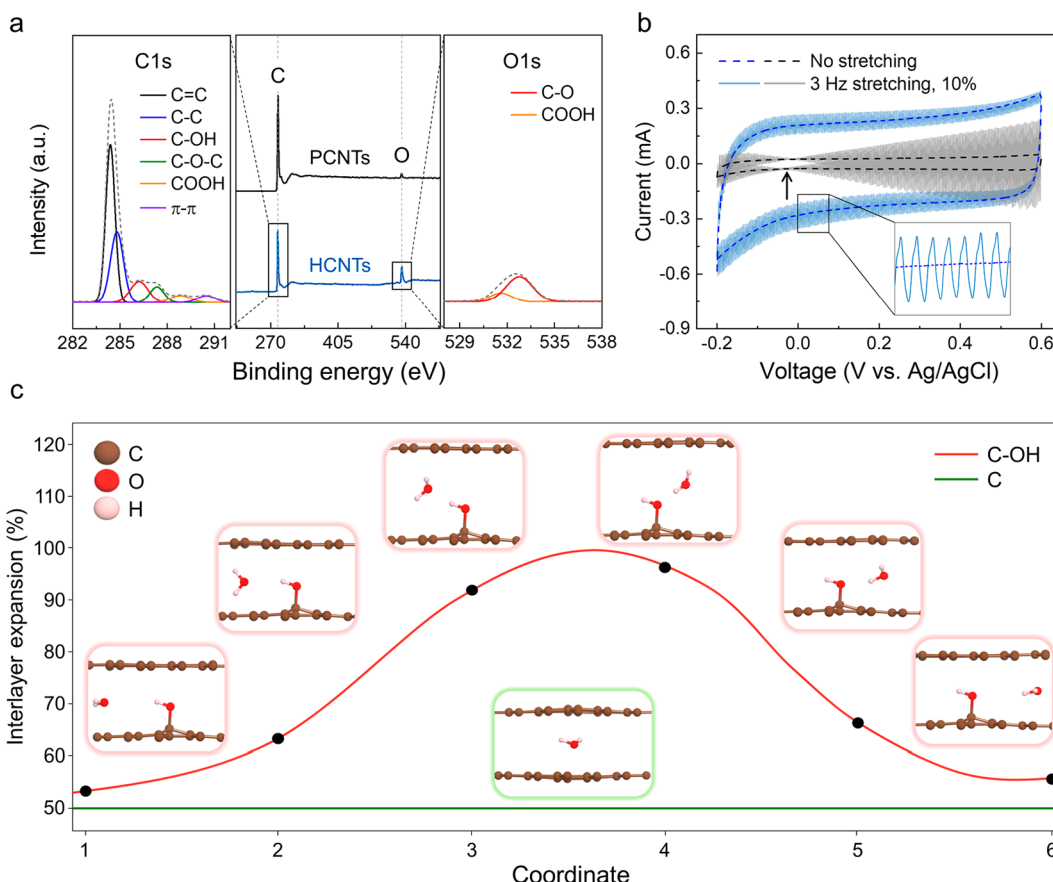


Figure 2. Water-driven volume expansion characterizations of HCNT coiled yarns. (a) X-ray photoelectron spectroscopy spectra of PCNTs and HCNTs. Magnified views on the left and right sides show high-resolution C1s and O1s spectra of HCNTs, respectively. (b) Measured piezoelectric spectroscopy (PECS) curves for a scan rate of 10 mV/s for PCNT (black) and HCNT (blue) coiled yarns in 0.1 M Na_2SO_4 electrolyte, respectively. Inset shows magnified PECS curve of HCNT coiled yarns during a 3 Hz sinusoidal stretch to 10% (solid line) and without deformation (dashed line). The potential of zero charge (PZC) point for the PCNT coiled yarns is indicated by an arrow. (c) Calculated expansion rate of interlayer distance of pristine and hydroxyl bilayer-graphene within snapshots of water molecule coordinates.

RESULTS AND DISCUSSION

Among the different kinds of botanical movements triggered by the supply or deprival of water, the motion strategy of seed awns of the *Erodium* species was mimicked because of their distinct hydraulic characteristics. The awns, which are composed of hygroscopically active and inactive layers, spontaneously twist in a dry state (Figure 1a).³¹ The mechanical energy stored in the awn is released as it untwists because of the volumetric change of the wet layer in the presence of water molecules (Figure 1b).³² These hygroscopic motions of awns are primarily exploited to screw seeds into the ground for germination.³³ Specifically, the helical deformation is significantly affected by the cell alignment and arrangement of cellulose microfibrils. Therefore, the aligned microstructures of awns have inspired us to develop helical yarn actuators powered by water molecules.

An aligned CNT sheet dry-drawn from a spinnable array was highly twisted and transformed into a coil-shaped pristine CNT (PCNT) yarn via a continuous spinning process to prepare a pre-twisted stored CNT yarn (Figure 1c).³⁴ The as-prepared yarn was then modified to an HCNT coiled yarn through facile ECO treatment for sensitive response to water molecules (for details, see Supporting Information (SI) Experimental Section). The electrochemical charge injection during ECO treatment produced a volume expansion of the

yarn (Figure S1), implying possible untwisting torsional actuation. Therefore, an engineered, hygroscopically active HCNT coiled yarn can actuate in the forward (untwisting) and reverse (retwisting) directions upon hydration and dehydration, respectively (Figure 1d), like the awns of *Erodium*. Moreover, the nanochannels formed between the CNT filaments provided a capillary force for efficient and rapid water infiltration (inset of Figure 1d). The HCNT yarns exhibited reversible and large volume changes during 100 repeated water absorption and desorption cycles (Figure 1e). On the basis of these results, the water-driven mechanical actuation of the HCNT yarns was investigated because the twisted yarn could generate untwisting actuation when its volume increases.^{9,29} Figure 1f shows the time dependence of the torsional stroke of the PCNT and HCNT yarns upon the alternation of hydration and dehydration. The rapid infiltration of water into the HCNT yarn resulted in an untwisting actuation (10.4 revolutions/cm; inset of Figure 1f, left image), whereas the PCNT yarn did not show any torsional stroke (inset of Figure 1f, right image).

The untwisting motion of the CNT yarn having a one-chiral McKibben structure is highly correlated with the volumetric expansion of the yarns,¹³ which can be considered a result of water infiltration based on the following two facts: (1) the nanochannels among the CNTs provide a large capacity for water absorption. (2) The oxygen content, which contributes

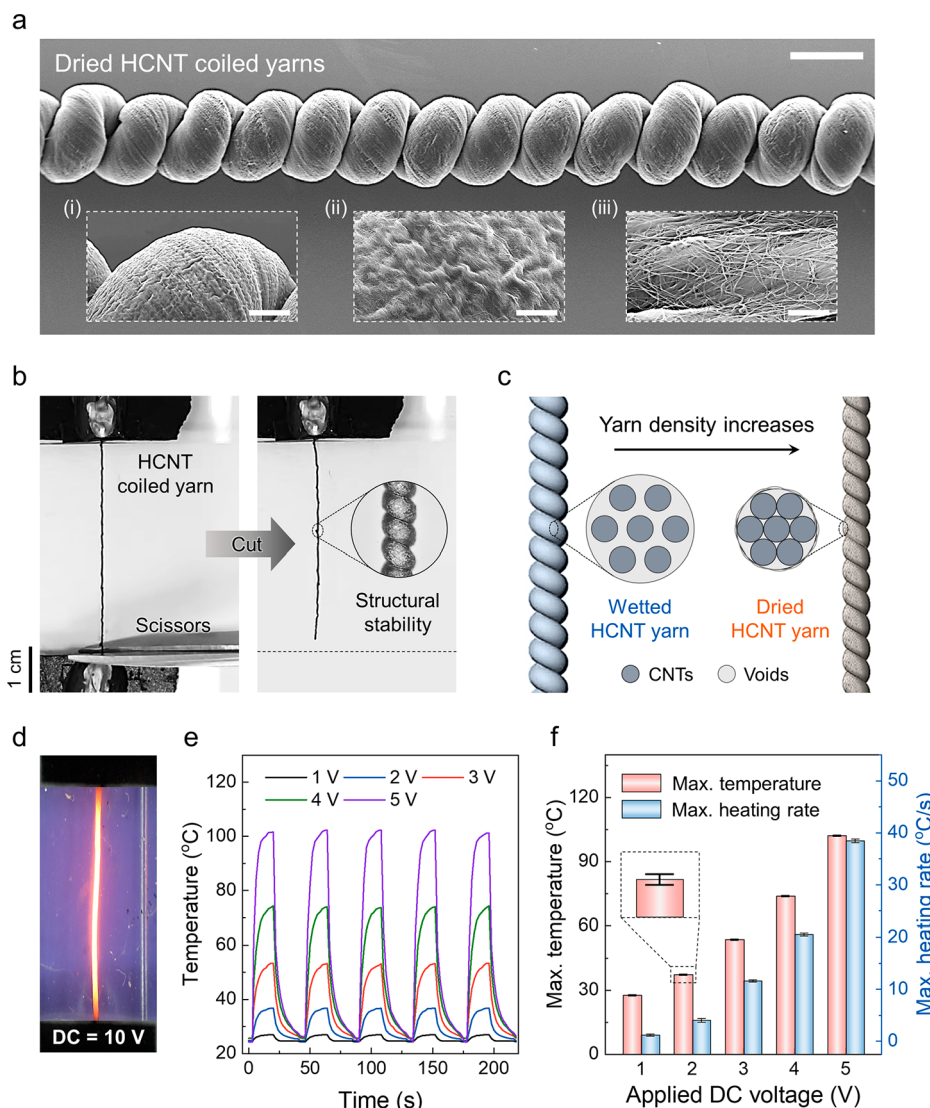


Figure 3. Morphological information and electric heating properties of dried HCNT coiled yarns. (a) Scanning electron microscopy (SEM) images of dried HCNT coiled yarns at low magnification (scale bar = 100 μ m). Insets (i, ii, and iii) show its various higher-magnification SEM images (scale bars: (i) = 30 μ m, (ii) = 10 μ m, and (iii) = 2 μ m). (b) Photographs show structural stability of HCNT coiled yarn in a free-standing state even when one end was cut off with scissors. (c) Schematics of density increase of HCNT coiled yarns after drying process with improved internanotube connections. (d) Three centimeters yarn segment producing light emission at a DC voltage of 10 V. (e) Yarn temperature–time curves at repetitive voltage applications of 1–5 V with on and off durations of approximately 22 s. (f) Maximal temperature and heating rate as a function of applied DC voltage. Inset shows enlarged image of the dashed area.

to high water interactivity, increases after ECO treatment according to the X-ray photoelectron spectroscopy (XPS) analysis (Figure 2a). The XPS survey spectra of the PCNTs and HCNTs reveal two dominant photoemission peaks: C1s (284.5 eV) and O1s (532.5 eV) (middle of Figure 2a). The oxygen and carbon (O/C) atomic ratios increased from 0.07 to 0.28 with increasing oxidation time, indicating that the contents of oxygenic groups on the CNT surfaces could be effectively controlled (Figure S2). The C1s peak (left side of Figure 2a) and O1s peak (right side of Figure 2a) were deconvoluted to investigate the detailed chemical composition of the HCNT yarns with Gaussian peak fitting,^{35,36} referring to the following bonds: C—C sp² (284.3 eV), C—C sp³ (284.8 eV), C—OH (286.2 eV), C—O—C (287.3 eV), and COOH (288.7 eV). The high-resolution O1s spectrum also shows noticeable peaks at 532.7 and 531.5 eV, which represent C—O and COOH bonds, respectively. These results agree with those

of previous studies.³⁶ Among the diverse types of oxygen-containing functional groups, C—O was predominant in the HCNTs. Another experimental proof for surface functionalization was obtained by investigating the potential of zero charge (PZC) of CNT coiled yarns immersed in an electrolyte by piezoelectric spectroscopy (PECS).³⁷ During PECS, the yarn was dynamically stretched with a sinusoidal tensile strain of 10% at 3 Hz (solid line) while conducting a cyclic voltammetry (CV) scan (dashed line) (Figure 2b). The PZC (the potential at which the stretch-induced current is minimized) was located at approximately -30 mV (vs. Ag/AgCl) for the PCNT coiled yarn (black), as indicated by the arrow. Although no obvious PZC point was located for the HCNT coiled yarn (blue) in the given potential range, PECS measured with an extended voltage window showed the largely shifted PZC at approximately 450 mV (vs. Ag/AgCl), as presented in Figure S3. This

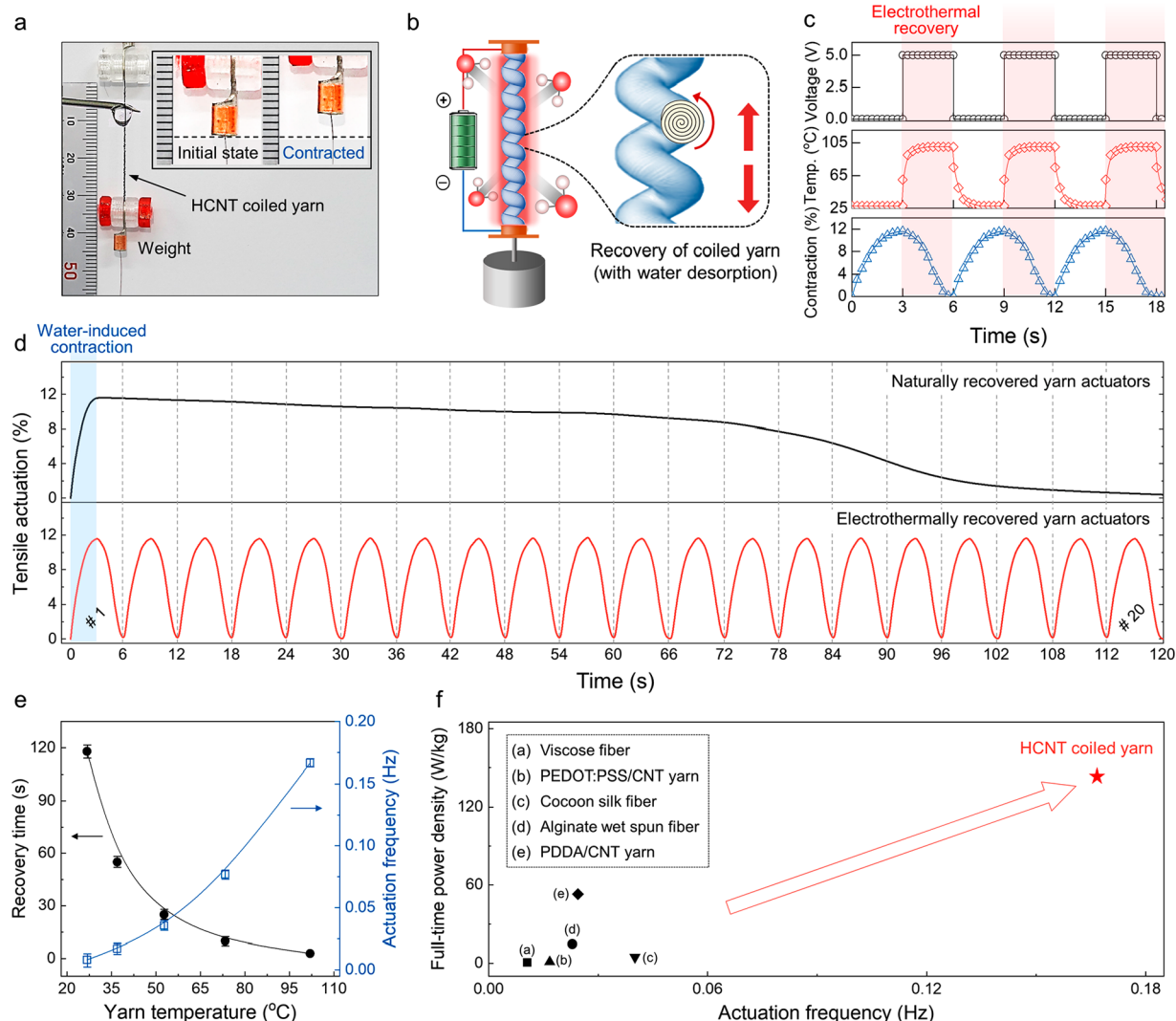


Figure 4. Fast electrothermal recovery of HCNT coiled yarn actuators with high-power density. (a) Photographs show an HCNT coiled yarn hydro-actuator while in contact with a water droplet under a 2 kPa isobaric load. Inset images show the weight, hanged by the coiled yarn, before and after water contraction. (b) Configuration for electrothermal recovery process of contracted coiled yarn hydro-actuators. The increase in the yarn temperature accelerates the desorption of water and leads to fast recovery in length with a yarn retwisting. (c) Time dependence of generated temperature on applied voltage and tensile stroke of coiled yarn hydro-actuators during water contraction and electrothermal recovery cycles (red-shaded region). (d) Tensile stroke versus time of coiled yarn hydro-actuator when actuated in consecutive water absorption (blue-shaded region) and desorption cycles without electric heating (upper panel) and with electric heating (lower panel). (e) Dependence of recovery time and actuation frequency on yarn temperature. (f) Full-time power densities versus actuation frequency of HCNT coiled yarn-based hydro-actuators and previously presented humidity- or water-responsive tensile actuators. Red star represents this work; black symbols represent previously reported results (see legend). Arrow represents the direction of property improvements compared with previous results.

PZC shift can be attributed to the surface polarity change of the functionalized coiled yarn after ECO treatment.¹⁹

The change in the interlayer distance of the CNTs during water absorption was calculated to explore the underlying reason for the water-activated yarn volume expansion (Figure 2c). A 4 × 4 bilayer graphene sheet model with 64 carbons was built for calculations to simplify the structure of PCNTs. When water molecules were introduced between the PCNT bilayers, the interlayer distance was expanded by only 50%. However, it increased from 54% to 97% as the water molecules approached the hydroxyl functional groups in the HCNTs. These results suggest that the interaction among hydroxyl functional groups and water molecules leads to the extraordinary radial volume expansion of HCNT coiled yarns.

An issue of irreversible untwisting without tethering in coiled yarns still remains unresolved because of the weak interfacial connection among neighboring CNTs in the yarns.³⁸ This problem can be particularly troublesome for actuation performance due to the possible loss of pre-stored twists. Interestingly, ECO-treated coiled yarn exhibits extraordinary structural stability with high wettability. As-coiled CNT yarns generally have a single-helix structure with regular helical loops exhibiting a constant bias angle, as shown in the scanning electron microscopy (SEM) images in Figure S4. The coil structure and initial bias angle were roughly maintained after ECO treatment and drying (Figure 3a-a-(i)). However, completely different microstructures can be seen, such as surface buckling (Figure 3a-(ii)) and condensed nanotube bundles (Figure 3a-(iii)). As a result, the dried HCNT coiled

yarns retained straight and negligibly untwisted even if one end was not tethered (Figure 3b), unlike the PCNT coiled yarns, which were entangled and snarled (Figure S5). This structural stability may be due to the microstructural transition after the ECO-driven volume expansion. Notably, the enhanced internanotube connections during yarn drying reduced the void space among nanotube bundles within yarns, resulting in increased yarn density (Figure 3c). As shown in Figure S6, the average outer diameter of the PCNT yarn was approximately 150 μm (density, $\rho = 0.85 \text{ g/cm}^3$). Following ECO treatment increased the diameter of the wetted HCNT yarn up to 170 μm ($\rho = 0.66 \text{ g/cm}^3$), which might be due to the water injection. Notably, the final diameter of totally dried HCNT yarn was 130 μm ($\rho = 1.13 \text{ g/cm}^3$), which is much lower than that of PCNT yarn. This stable coiled yarn construction is significantly meaningful because it can allow the actuator operation without unwanted untwisting before mechanical actuation.

Furthermore, the electrical and mechanical properties of the HCNT coiled yarns were characterized. The nearly linear $I-V$ curve indicates the low and stable resistance of the HCNT coiled yarn (Figure S7). The stress-strain curves of the HCNT coiled yarns show that the elongation strain before fracture was approximately 105%, with an ultimate tensile strength of 29.2 MPa and a modulus of 27.8 MPa (Figure S8). Although the strength and modulus were slightly lower than those of the PCNT coiled yarns (35.5 and 34.4 MPa, respectively), fracture elongation was largely retained.

In addition, when 10 V was applied, stable and uniform light emission was observed because of the high electrical conductivity of the HCNT coiled yarns (approximately $3.63 \times 10^4 \text{ S/m}$; Figure 3d). Moreover, their electric heating properties were investigated by tracking the temperature change over time (Figure 3e). No increase in apparent temperature was observed at an input voltage of 1 V. However, 2 V generated a maximal temperature of approximately 37 °C, which further uniformly increased to 53, 74, and 102 °C at 3, 4, and 5 V, respectively. Furthermore, the stable cyclic heating performance was demonstrated during 100 repeated voltage application (Figure S9). Figure 3f shows the dependence of the generated temperature (left axis) and maximal heating rate (right axis) of the yarns on the applied DC voltage. The maximal temperature and applied voltage showed a quasi-linear relationship between 1 and 5 V. A similar trend was observed for the maximal heating rate within the investigated voltage range, showing a high value of 39 °C/s at 5 V. This behavior can be attributed to their high thermal conductivity³⁹ and large specific surface area.⁴⁰

An outstanding feature of electrically heatable HCNT coiled yarns is rapidly recoverable hydro-actuation through the application of a DC voltage. A 30 mm long coiled yarn actuator was isobarically loaded with a torsionally tethered weight, preserving the total number of turns in the yarn during actuation (Figure 4a). Therefore, the changes in coiled yarn twist by volume expansion only allowed contraction in coil length without net rotation because untwist-generated torsional torque could pull adjacent coils together.²⁹ Highly stable tensile contraction for the HCNT coiled yarn was observed after hydration, as shown in the inset of Figure 4a. The absorbed water molecules caused the yarn to expand radially (Figure S10), thereby causing the yarn to untwist and contract axially. The effect of the applied load on the tensile stroke and work capacity of the HCNT coiled yarn actuator was also

investigated (Figure S11). The tensile stroke initially increased from 10.48% to 12.25% and then decreased to 7.47% with increasing load. Furthermore, the work capacity reached a peak of 863 J/kg during yarn contraction at 11.8 MPa stress, which is approximately 22 times higher than that of mammalian skeletal muscles.⁴¹ Please note that isotonic tensile strokes were characterized unless specified otherwise.

This coil structure-based tensile actuation is well-known for its good reversibility. However, most humidity- or water-driven tensile actuators show delayed recovery time compared to the contraction time because of the slow evaporation rate of water under standard atmospheric conditions⁴² and the reduced stiffness⁴³ in the water-swollen state. One way to reduce dramatically the desorption time is to generate heat inside the yarn using electric heating to accelerate the evaporation of water, that is, the increased yarn temperature can lead to fast dehydration and recovery, irrespective of the external environmental conditions. Figure 4b depicts the schematic configuration for electrothermal recovery. Two electrodes were connected at the top and bottom ends of an HCNT coiled yarn with constant stress. The heat generated after the application of a voltage increased the yarn temperature, thereby rapidly ejecting water molecules that had infiltrated into the yarn during contraction. The water desorption process initialized the expanded volume of the yarn actuator. Such volume recovery can cause the yarn to retwist, leading to both intercoil separation and length elongation. Figure 4c shows the time-dependent tensile stroke of the yarn actuator subjected to 11.8 MPa pre-tension. The tensile stroke gradually reached 12.25% after delivering 3 s of a water drop. Subsequently, the yarn actuators gradually returned to the original state within 3 s when a 10 Hz, 0–5 V square wave was applied with a 50% duty cycle.

The yarn actuators were consecutively hydrated and dehydrated under two different yarn temperatures, ambient temperature and electrically heated temperature, to demonstrate their fast electrothermal recovery. The resulting time dependences of the tensile actuation were compared (Figure 4d). A total-cycle time of the yarn actuator was reduced by up to 95% compared to the time taken in natural conditions without electric heating. More specifically, the electrothermally recovered yarn actuators quickly repeated 20 cycles during the investigated time of 120 s; by contrast, the naturally recovered yarn actuators operated only once. The HCNT yarn actuator also showed stable long-term performance during 100 repeated water contraction and electric heating cycles (Figure S12). Figure 4e shows the recovery time and actuation frequency versus the generated yarn temperature when 1–5 V was applied. The recovery time is inversely proportional to the yarn temperature; therefore, the corresponding frequency increased from 0.008 to 0.17 Hz when the yarn temperature increased from 26 to 102 °C. This high frequency can be advantageous for constructing high-power hydro-actuators. The actuation frequency and full-time power density of the HCNT coiled yarn actuators were plotted and compared with those of previously presented tensile hydro-actuators (Figure 4f). Considering the total cycle time, frequency and full-time power density were much higher (0.17 Hz and 143.8 W/kg) than previously reported results: (a) the viscose fiber hydro-actuator (0.01 Hz and 1.2 W/kg),²⁵ (b) PEDOT:PSS/CNT yarn hydro-actuator (0.02 Hz and 1.6 W/kg),²¹ (c) cocoon silk fiber hydro-actuator (0.04 Hz and 2.9 W/kg),⁸ (d) Alginate wet spun fiber hydro-actuator (0.02 Hz and 14.7 W/kg),²⁶ and

(e) PDPA/CNT yarn hydro-actuator (0.02 Hz and 52.9 W/kg).²² Unless the specific values were noted in previous reports, the total cycle time was obtained from the actuation graph and then used to calculate the full-time power density. Further comparisons of the actuation performance of the HCNT coiled yarn actuator with other tensile hydro-actuators are provided in Table S1.

CONCLUSION

In summary, an electrothermally recoverable high-power hydro-actuator was developed via the biomimetic design of pre-twisted and water-responsive CNT yarns. The HCNT coiled yarns were fabricated by introducing giant twists into CNT sheets, followed by ECO treatment. The resulting yarns showed extraordinary structural stability without the possible loss of pre-stored twists because of the enhanced internanotube connections and yarn density. The HCNT coiled yarn hydro-actuators provided a maximal contractile work of 863 J/kg at 11.8 MPa stress when powered by water absorption. Notably, the excellent electric heating properties even after ECO treatment enabled the accelerated evaporation of water absorbed inside the yarn, dramatically reducing a total-cycle time by up to 95% compared to the time taken in natural conditions. Finally, the electrothermally recoverable hydro-actuators exhibited a high actuation frequency (0.17 Hz) and full-time power density (143.8 W/kg). These achievements suggest that presented high-power hydro-actuators can be used in diverse applications, such as soft robotics, prosthetics, and bionic devices.

ASSOCIATED CONTENT

Supporting Information

The Supporting Information is available free of charge at <https://pubs.acs.org/doi/10.1021/acs.nanolett.2c00250>.

Experimental section; photograph of electrochemical charge injection-induced volume expansion of CNT coiled yarns; surface analysis of HCNT yarns by XPS and PECS; SEM images and photographs of PCNT coiled yarns; characterization of yarn density; electrical, mechanical, and electrothermal properties of HCNT coiled yarns; tensile actuation performances of HCNT coiled yarn actuators; long-term cycling test of tensile actuation; comparison table of actuation performances ([PDF](#))

AUTHOR INFORMATION

Corresponding Authors

Sungwoo Chun – Department of Electronics and Information Engineering, Korea University, Sejong 30019, Republic of Korea; Email: swchun127129@korea.ac.kr

Changsoon Choi – Department of Energy and Materials Engineering, Dongguk University-Seoul, Seoul 04620, Republic of Korea; orcid.org/0000-0003-4456-4548; Email: cschoi84@dongguk.edu

Authors

Wonkyeong Son – Department of Energy and Materials Engineering, Dongguk University-Seoul, Seoul 04620, Republic of Korea; Department of Energy Science, Sungkyunkwan University, Suwon 16419, Republic of Korea

Jae Myeong Lee – Department of Energy and Materials Engineering, Dongguk University-Seoul, Seoul 04620, Republic of Korea

Shi Hyeong Kim – Advanced Textile R&D Department, Korea Institute of Industrial Technology (KITECH), Ansan 15588, South Korea

Hyeon Woo Kim – Convergence Technology Division, Korea Institute of Ceramic Engineering and Technology (KICET), Jinju-si 52851, Republic of Korea; Division of Materials Science and Engineering, Hanyang University, Seoul 04736, Republic of Korea

Sung Beom Cho – Convergence Technology Division, Korea Institute of Ceramic Engineering and Technology (KICET), Jinju-si 52851, Republic of Korea; orcid.org/0000-0002-3151-0113

Dongseok Suh – Department of Energy Science, Sungkyunkwan University, Suwon 16419, Republic of Korea; orcid.org/0000-0002-0392-3391

Complete contact information is available at:
<https://pubs.acs.org/10.1021/acs.nanolett.2c00250>

Author Contributions

W.S. and J.M.L. equally contributed to this work.

Author Contributions

W.S., S.C., D.S., and C.C. conceived the idea and performed the experiments. J.M.L. and S.H.K. analyzed the experimental results. H.W.K. and S.B.C. performed the simulations. All authors contributed to writing the manuscript.

Notes

The authors declare no competing financial interest.

ACKNOWLEDGMENTS

This work was supported by the Korea Institute of Industrial Technology (KITECH EH220002) and the Basic Science Research Programs through the National Research Foundation of Korea (NRF-2017R1A6A3A04004987 and NRF-2021R1A2C2005281).

REFERENCES

- Spinks, G. M. Advanced Actuator Materials Powered by Biomimetic Helical Fiber Topologies. *Adv. Mater.* **2020**, *32* (18), No. 1904093.
- Chen, P.; Xu, Y.; He, S.; Sun, X.; Pan, S.; Deng, J.; Chen, D.; Peng, H. Hierarchically Arranged Helical Fibre Actuators Driven by Solvents and Vapours. *Nat. Nanotechnol.* **2015**, *10* (12), 1077–1084.
- Liu, Y. Q.; Chen, Z. D.; Han, D. D.; Mao, J. W.; Ma, J. N.; Zhang, Y. L.; Sun, H. B. Bioinspired Soft Robots Based on the Moisture-Responsive Graphene Oxide. *Adv. Sci.* **2021**, *8* (10), 2002464.
- Ha, J.; Choi, S. M.; Shin, B.; Lee, M.; Jung, W.; Kim, H.-Y. Hygroresponsive Coiling of Seed Awns and Soft Actuators. *Extreme. Mech. Lett.* **2020**, *38*, 100746.
- Shin, B.; Ha, J.; Lee, M.; Park, K.; Park, G. H.; Choi, T. H.; Cho, K.-J.; Kim, H.-Y. Hygrobot: A Self-Locomotive Ratcheted Actuator Powered by Environmental Humidity. *Sci. Robot.* **2018**, *3* (14), No. eaar2629.
- Cheng, Y.; Wang, R.; Chan, K. H.; Lu, X.; Sun, J.; Ho, G. W. A Biomimetic Conductive Tendril for Ultrastretchable and Integratable Electronics, Muscles, and Sensors. *ACS Nano* **2018**, *12* (4), 3898–3907.
- Liu, Y. Q.; Chen, Z. D.; Han, D. D.; Mao, J. W.; Ma, J. N.; Zhang, Y. L.; Sun, H. B. Bioinspired Soft Robots Based on the Moisture-Responsive Graphene Oxide. *Adv. Sci.* **2021**, *8* (10), 2002464.

- (8) Jia, T.; Wang, Y.; Dou, Y.; Li, Y.; Jung de Andrade, M.; Wang, R.; Fang, S.; Li, J.; Yu, Z.; Qiao, R.; Liu, Z.; Cheng, Y.; Su, Y.; Minary-Jolandan, M.; Baughman, R. H.; Qian, D.; Liu, Z. Moisture Sensitive Smart Yarns and Textiles from Self-Balanced Silk Fiber Muscles. *Adv. Funct. Mater.* **2019**, *29* (18), 1808241.
- (9) Lin, S.; Wang, Z.; Chen, X.; Ren, J.; Ling, S. Ultrastrong and Highly Sensitive Fiber Microactuators Constructed by Force-Reeled Silks. *Adv. Sci.* **2020**, *7* (6), 1902743.
- (10) Hu, J.; Irfan Iqbal, M.; Sun, F. Wool Can Be Cool: Water-Actuating Woolen Knitwear for Both Hot and Cold. *Adv. Funct. Mater.* **2020**, *30* (51), 2005033.
- (11) Yang, X.; Wang, W.; Miao, M. Moisture-Responsive Natural Fiber Coil-Structured Artificial Muscles. *ACS Appl. Mater. Interfaces* **2018**, *10* (38), 32256–32264.
- (12) Leng, X.; Hu, X.; Zhao, W.; An, B.; Zhou, X.; Liu, Z. Recent Advances in Twisted-Fiber Artificial Muscles. *Adv. Intell. Syst.* **2021**, *3* (5), 2000185.
- (13) Foroughi, J.; Spinks, G. M.; Wallace, G. G.; Oh, J.; Kozlov, M. E.; Fang, S.; Mirfakhrai, T.; Madden, J. D. W.; Shin, M. K.; Kim, S. J.; Baughman, R. H. Torsional Carbon Nanotube Artificial Muscles. *Science* **2011**, *334* (6055), 494–497.
- (14) Lima, M. D.; Li, N.; Jung de Andrade, M.; Fang, S.; Oh, J.; Spinks, G. M.; Kozlov, M. E.; Haines, C. S.; Suh, D.; Foroughi, J.; Kim, S. J.; Chen, Y.; Ware, T.; Shin, M. K.; Machado, L. D.; Fonseca, A. F.; Madden, J. D. W.; Voit, W. E.; Galvao, D. S.; Baughman, R. H. Electrically, Chemically, and Photonically Powered Torsional and Tensile Actuation of Hybrid Carbon Nanotube Yarn Muscles. *Science* **2012**, *338* (6109), 928–932.
- (15) Chun, K. Y.; Kim, S. H.; Shin, M. K.; Kwon, C. H.; Park, J.; Kim, Y. T.; Spinks, G. M.; Lima, M. D.; Haines, C. S.; Baughman, R. H.; Kim, S. J. Hybrid Carbon Nanotube Yarn Artificial Muscle Inspired by Spider Dragline Silk. *Nat. Commun.* **2014**, *5*, 3322.
- (16) Lee, J. A.; Kim, Y. T.; Spinks, G. M.; Suh, D.; Lepro, X.; Lima, M. D.; Baughman, R. H.; Kim, S. J. All-Solid-State Carbon Nanotube Torsional and Tensile Artificial Muscles. *Nano Lett.* **2014**, *14* (5), 2664–2669.
- (17) Chen, P.; He, S.; Xu, Y.; Sun, X.; Peng, H. Electromechanical Actuator Ribbons Driven by Electrically Conducting Spring-Like Fibers. *Adv. Mater.* **2015**, *27* (34), 4982–4988.
- (18) Qiao, J.; Di, J.; Zhou, S.; Jin, K.; Zeng, S.; Li, N.; Fang, S.; Song, Y.; Li, M.; Baughman, R. H.; Li, Q. Large-Stroke Electrochemical Carbon Nanotube/Graphene Hybrid Yarn Muscles. *Small* **2018**, *14* (38), 1801883.
- (19) Chu, H.; Hu, X.; Wang, Z.; Mu, J.; Li, N.; Zhou, X.; Fang, S.; Haines, C. S.; Park, J. W.; Qin, S.; Yuan, N.; Xu, J.; Tawfick, S.; Kim, H.; Conlin, P.; Cho, M.; Cho, K.; Oh, J.; Nielsen, S.; Alberto, K. A.; Razal, J. M.; Foroughi, J.; Spinks, G. M.; Kim, S. J.; Ding, J.; Leng, J.; Baughman, R. H. Unipolar Stroke, Electroosmotic Pump Carbon Nanotube Yarn Muscles. *Science* **2021**, *371* (6528), 494–498.
- (20) Dong, Y.; Wang, L.; Wang, J.; Wang, S.; Wang, Y.; Jin, D.; Chen, P.; Du, W.; Zhang, L.; Liu, B. F. Graphene-Based Helical Micromotors Constructed by "Microscale Liquid Rope-Coil Effect" with Microfluidics. *ACS Nano* **2020**, *14* (12), 16600–16613.
- (21) Gu, X.; Fan, Q.; Yang, F.; Cai, L.; Zhang, N.; Zhou, W.; Zhou, W.; Xie, S. Hydro-Actuation of Hybrid Carbon Nanotube Yarn Muscles. *Nanoscale* **2016**, *8* (41), 17881–17886.
- (22) Kim, S. H.; Kwon, C. H.; Park, K.; Mun, T. J.; Lepró, X.; Baughman, R. H.; Spinks, G. M.; Kim, S. J. Bio-Inspired, Moisture-Powered Hybrid Carbon Nanotube Yarn Muscles. *Sci. Rep.* **2016**, *6*, 23016.
- (23) He, S.; Chen, P.; Qiu, L.; Wang, B.; Sun, X.; Xu, Y.; Peng, H. A Mechanically Actuating Carbon-Nanotube Fiber in Response to Water and Moisture. *Angew. Chem.* **2015**, *127* (49), 15093–15097.
- (24) Cheng, H.; Hu, Y.; Zhao, F.; Dong, Z.; Wang, Y.; Chen, N.; Zhang, Z.; Qu, L. Moisture-Activated Torsional Graphene-Fiber Motor. *Adv. Mater.* **2014**, *26* (18), 2909–2913.
- (25) Li, Y.; Miao, M. Water-Responsive Artificial Muscles from Commercial Viscose Fibers without Chemical Treatment. *Mater. Res. Lett.* **2020**, *8* (6), 232–238.
- (26) Wang, W.; Xiang, C.; Liu, Q.; Li, M.; Zhong, W.; Yan, K.; Wang, D. Natural Alginate Fiber-based Actuator Driven by Water or Moisture for Energy Harvesting and Smart Controller Applications. *J. Mater. Chem. A* **2018**, *6* (45), 22599–22608.
- (27) Agnarsson, I.; Dhinojwala, A.; Sahni, V.; Blackledge, T. A. Spider Silk as a Novel High Performance Biomimetic Muscle Driven by Humidity. *J. Exp. Biol.* **2009**, *212* (13), 1990–1994.
- (28) Wang, Y.; Wang, Z.; Lu, Z.; de Andrade, M. J.; Fang, S.; Zhang, Z.; Wu, J.; Baughman, R. H. Humidity- and Water-Responsive Torsional and Contractile Lotus Fiber Yarn Artificial Muscles. *ACS Appl. Mater. Interfaces* **2021**, *13* (5), 6642–6649.
- (29) Moraitis, G.; Špitálský, Z.; Ravani, F.; Siokou, A.; Galiotis, C. Electrochemical Oxidation of Multi-Wall Carbon Nanotubes. *Carbon* **2011**, *49* (8), 2702–2708.
- (30) Ye, J.-S.; Liu, X.; Cui, H. F.; Zhang, W.-D.; Sheu, F.-S.; Lim, T. M. Electrochemical Oxidation of Multi-Walled Carbon Nanotubes and its Application to Electrochemical Double Layer Capacitors. *Electrochim. Commun.* **2005**, *7* (3), 249–255.
- (31) Aharoni, H.; Abraham, Y.; Elbaum, R.; Sharon, E.; Kupferman, R. Emergence of Spontaneous Twist and Curvature in Non-Euclidean Rods: Application to Erodium Plant Cells. *Phys. Rev. Lett.* **2012**, *108* (23), 238106.
- (32) Jung, W.; Choi, S. M.; Kim, W.; Kim, H.-Y. Reduction of Granular Drag Inspired by Self-Burrowing Rotary Seeds. *Phys. Fluids* **2017**, *29* (4), 041702.
- (33) Evangelista, D.; Hotton, S.; Dumais, J. The Mechanics of Explosive Dispersal and Self-Burial in the Seeds of the Filaree, Erodium Cicutarium (Geraniaceae). *J. Exp. Biol.* **2011**, *214* (4), 521–529.
- (34) Qiu, L.-b.; Sun, X.-m.; Yang, Z.-b.; Guo, W.; Peng, H. Preparation and Application of Aligned Carbon Nanotube/Polymer Composite Material. *Acta Chim. Sin.* **2012**, *70* (14), 1523–1532.
- (35) Shao, Y.; Xu, F.; Marriam, I.; Liu, W.; Gao, Z.; Qiu, Y. Quasi-Static and Dynamic Interfacial Evaluations of Plasma Functionalized Carbon Nanotube Fiber. *Appl. Surf. Sci.* **2019**, *465*, 795–801.
- (36) Adusei, P. K.; Gbordzoe, S.; Kanakaraj, S. N.; Hsieh, Y.-Y.; Alvarez, N. T.; Fang, Y.; Johnson, K.; McConnell, C.; Shanov, V. Fabrication and Study of Supercapacitor Electrodes based on Oxygen Plasma Functionalized Carbon Nanotube Fibers. *J. Energy Chem.* **2020**, *40*, 120–131.
- (37) Kim, S. H.; Haines, C. S.; Li, N.; Kim, K. J.; Mun, T. J.; Choi, C.; Di, J.; Oh, Y. J.; Oviedo, J. P.; Bykova, J.; Fang, S.; Jiang, N.; Liu, Z.; Wang, R.; Kumar, P.; Qiao, R.; Priya, S.; Cho, K.; Kim, M.; Lucas, M. S.; Drummy, L. F.; Maruyama, B.; Lee, D. Y.; Lepro, X.; Gao, E.; Albarq, D.; Oballe-Robles, R.; Kim, S. J.; Baughman, R. H. Harvesting Electrical Energy from Carbon Nanotube Yarn Twist. *Science* **2017**, *357* (6353), 773–778.
- (38) Fillette, T.; Espinosa, H. D. Multi-Scale Mechanical Improvement Produced in Carbon Nanotube Fibers by Irradiation Cross-Linking. *Carbon* **2013**, *S6*, 1–11.
- (39) Liu, P.; Fan, Z.; Mikhalkan, A.; Tran, T. Q.; Jewell, D.; Duong, H. M.; Marconnet, A. M. Continuous Carbon Nanotube-Based Fibers and Films for Applications Requiring Enhanced Heat Dissipation. *ACS Appl. Mater. Interfaces* **2016**, *8* (27), 17461–17471.
- (40) Liu, P.; Liu, L.; Wei, Y.; Liu, K.; Chen, Z.; Jiang, K.; Li, Q.; Fan, S. Fast High-Temperature Response of Carbon Nanotube Film and Its Application as an Incandescent Display. *Adv. Mater.* **2009**, *21* (35), 3563–3566.
- (41) Mirvakili, S. M.; Hunter, I. W. Artificial Muscles: Mechanisms, Applications, and Challenges. *Adv. Mater.* **2018**, *30* (6), 1704407.
- (42) Tang, R.; Etzion, Y. Comparative Studies on the Water Evaporation Rate from a Wetted Surface and that from a Free Water Surface. *Building and Environment* **2004**, *39* (1), 77–86.
- (43) Liu, Y.; Das, N. C.; Wang, H.; Zhang, G.; Cho, J.; Hong, K.; Eres, G.; Uhrig, D. Aligned Carbon Nanotube Polymer Composites. ASME International Mechanical Engineering Congress and Exposition; Seattle, WA; November 11–15, 2007; ASME, 2007; Paper No. IMECE2007-43776 2007; pp 55–58.

(44) EBS Documentary. "GREEN ANIMAL_#003" [Video file]. YouTube, November 30, 2016. <https://www.youtube.com/watch?v=O81HrFRmDqA> (accessed 2020-07-21).

□ Recommended by ACS

Enhanced Hydro-Actuation and Capacitance of Electrochemically Inner-Bundle-Activated Carbon Nanotube Yarns

Wonkyeong Son, Changsoon Choi, *et al.*

FEBRUARY 28, 2023

ACS APPLIED MATERIALS & INTERFACES

READ ↗

Selective Laser Sintering for Electrically Conductive Poly(dimethylsiloxane) Composites with Self-Healing Lattice Structures

Xue Li, Hesheng Xia, *et al.*

APRIL 03, 2023

ACS APPLIED POLYMER MATERIALS

READ ↗

Rapid Resistive Heating in Graphene/Carbon Nanotube Hybrid Films for De-icing Applications

Christos Kostaras, Konstantinos Dassios, *et al.*

MARCH 16, 2023

ACS APPLIED NANO MATERIALS

READ ↗

Stretchable Conductive Tubular Composites Based on Braided Carbon Nanotube Yarns with an Elastomer Matrix

Avia J. Bar, Samuel Kenig, *et al.*

NOVEMBER 07, 2022

ACS OMEGA

READ ↗

[Get More Suggestions >](#)